ELSEVIER

Polymer 40 (1999) 1223–1231

polymer

Crystallization kinetics of poly(ether ether ketone) (PEEK) from its metastable melt

Susheng Tan, Aihua Su[1], Jun Luo, Enle Zhou*

Polymer Physics Laboratory, Changchun Institute of Applied Chemistry, Chinese Academy of Sciences, Changchun 130022, People's Republic of China

Received 5 November 1997; revised 23 February 1998; accepted 23 March 1998

Abstract

After isothermal crystallization of the amorphous poly(ether ether ketone), double endothermic behaviour can be found through differential scanning calorimetry experiments. During the heating scan of semicrystalline PEEK, a metastable melt, which comes from the melt of the thinner lamellar crystal populations, can be obtained between these two endotherms. The metastable melt can recrystallize immediately just above the lower melting temperature and form slightly thicker lamellae than the original ones. The thickness and the perfection depend upon the crystallization time and the crystallization temperature. By comparing the TEM morphological observations of the samples before and after partial melting, it can be shown that lamellar crystals, having different thermodynamic stability, form during isothermal crystallization. After partial melting, only the type of lamellar crystal exhibiting the higher thermodynamic stability remains. Wide angle X-ray diffraction measurements shows a slightly change in the crystallinity of the samples before and after the partial melting. Small angle X-ray scattering results exhibit a change in the long period of the lamellar crystals before and after the partial melting process. The crystallization kinetics of the metastable melt can be determined by means of differential scanning calorimetry. The kinetic analysis showed that the isothermal crystallization of the metastable PEEK melt proceeds with an Avrami exponent of $n = 1.0 \sim 1.4$, reflecting that probably one-dimensional or an irregular line growth of the crystal occurred between the existing main lamellae with heterogeneous nucleation.

Keywords: Poly(ether ether ketone); Crystal morphology; Metastable melt

1. Introduction

There has been a great deal of interest in the double or multiple melting behaviour of thermoplastic semicrystalline polymers, which have been previously crystallized isothermally. In such a case, two endothermic melting peaks, a minor low-temperature peak a few degrees above the prior crystallization temperature and a major high-temperature peak, are observed in subsequent differential scanning calorimetry (d.s.c.) heating scans [1–14]. Extensive studies on the origin of the low endotherm have been performed using PEEK. Several models have been proposed to account for these low endotherms [4,5,15–21]. The dual lamellar thickness model first proposed by Cebe et al. [7] has been proven to be more acceptable than others. They assume that thinner lamellae are present in separate stacks between the thicker lamellae. In the early stage of crystallization, lamellar stacks consisting of thicker lamellae form from the melt and/or the amorphous state and the region in-between these lamellar stacks simultaneously creates amorphous areas. Later, lamellar stacks with thinner lamellae form in these amorphous areas. These stacks have the same amorphous layer thickness, but exhibit a different long period. The existence of these dual lamellar thickness in different stacks could be related to the double melting behaviour.

Whichever of the models we use, the low-temperature peak seems to result from the melting of the existing lamellae in the semicrystalline polymer samples. In such a case, the melt is far from the equilibrium state, so it is metastable or non-equilibrium. Only if there is enough time to rearrange the chains would the metastable melt recrystallize immediately just above the melting temperature. Thus, investigation of the crystallization kinetics of the metastable melts may help us explain the growth model of crystallites.

In this present work, the double endothermic behaviour and the corresponding crystal morphology of PEEK are

* Corresponding author.
[1] Permanent address: College of Science, Jilin University of Technology, Changchun 130022, People's Republic of China

0032-3861/98/$ - see front matter
PII S0032-3861(98)00275-4

studied using d.s.c., TEM, WAXD and SAXS measurements. The isothermal-crystallization kinetics of the metastable PEEK melt by means of the classic Avrami theory of phase transformation are also carried out.

2. Experimental

2.1. Materials and preparations

Amorphous poly(ether ether ketone) (PEEK) was obtained as a powder from ICI Co. The number average molecular weight is 14 000 g mol^{-1}. The amorphous films were obtained by hot mould at 10 MPa and 400°C for several minutes, then quenched into ice-water. The amorphous films were subjected to isothermal cold crystallization at 220°C for 24 h, then post-annealed at other higher temperatures, respectively, for different times. These samples were prepared for using in d.s.c. measurements. They all have the same thermal history as those used in TEM observations, WAXD and SAXS measurements.

Thin PEEK films were prepared for TEM observations by casting a 0.05% (w/w) PEEK–tetrachloroethane/*p*-chlorophenol solution on to carbon-coated mica. The solvent was subsequently evaporated under vacuum. The samples were heated to about 30°C above the equilibrium melting temperature for several minutes, and then quenched into liquid nitrogen to obtain the amorphous thin films. After cold crystallization at 220°C, the films were stripped, floated on to a water surface, and picked up on to copper grids.

A similar partial melting process was also carried out to study the correspondence between the double endotherms and crystal morphology as mentioned by Bassett et al. [8]. After completing isothermal crystallization, the crystallized samples were heated from room temperature to 245°C, which is in-between the low and the high endothermic peaks, and then quenched into liquid nitrogen.

2.2. Differential scanning calorimetry measurements

The post-annealing and crystallization kinetics of semicrystalline PEEK were investigated using d.s.c. A power-compensated differential scanning calorimeter, Perkin-Elmer DSC-7 series, was used in the present work. The temperature and heats of melting and crystallization were calibrated with indium and zinc standards. A nitrogen purge was used throughout. Isothermal crystallization from the metastable state was brought to completion by heating the semicrystalline PEEK annealed at 220°C for 24 h to the presetting temperatures with 20°C min^{-1} and then recording the time spectra at these temperatures. We assume that the relative extent of crystallinity which developed at time t, X_t, was

$$X_t = \int_0^t (\mathrm{d}H_c/\mathrm{d}t)\mathrm{d}t / \int_0^\infty (\mathrm{d}H_t/\mathrm{d}t)dt \quad (1)$$

in which $\mathrm{d}H_c/\mathrm{d}t$ is the heat evolution rate at time t, due to crystallization. $\int_0^\infty (\mathrm{d}H_t/\mathrm{d}t)\mathrm{d}t$ is the total area under the crystallization exotherm at the crystallization temperature T_c. The discussion of the calculation of the relative crystallinity can be seen in the text.

2.3. TEM observations

The specimens were examined with shadowing with a JEOL JEM-2010EX electron microscope (LaB_6 filament) which was operated at 200 kV with a side-entry goniometer and a liquid nitrogen anti-contamination trap. The images were recorded on photographic plates. Electron diffraction measurement was made using the selected area diffraction method. Electron diffraction diagrams were calibrated with gold.

2.4. WAXD and SAXS measurements

Wide angle X-ray diffraction was carried out for all samples in a Philips Model PW1700 automatic diffractometer in the reflection mode at 40 kV and 30 mA. The X-ray beam was monochromatized using a graphite crystal. The 2θ angle region ranged between 5° and 45° with a scanning rate of 0.1° min^{-1}. The step of 0.05° and the period of 4 s per step were used throughout the experiments. The diffraction peak positions and widths observed from WAXD experiments were carefully calibrated with silicon crystals.

SAXS measurement was carried out on the same X-ray diffractometer equipped with a Kratky small-angle X-ray camera and a sample-to-detector distance of 200 mm. The measurements were performed with a CuK_α radiation source. SAXS data were recorded with a one-dimensional position detector and allowed to add up over 10^5 in order to reduce the statistical errors. The measured intensity was corrected for background scattering and desmeared with a method proposed by Strobl [22].

The thermal history of the PEEK thin films using for WAXD and SAXS measurements were the same as the TEM observations.

3. Results and discussion

3.1. Double melting behaviour revisited

As described in the experimental section, all samples were first subjected to cold crystallization at 220°C for 24 h. The d.s.c. scans of the PEEK samples which were subjected to post-annealing at different temperatures for 30 min are shown in Fig. 1. In addition to the high temperature melting peak, another minor peak appeared several degrees just above the post-annealing temperature. In fact, the appearance of the d.s.c. traces is very similar to that expected by isothermally cold crystallization at the annealing temperature. The shape of the main upper peak remains

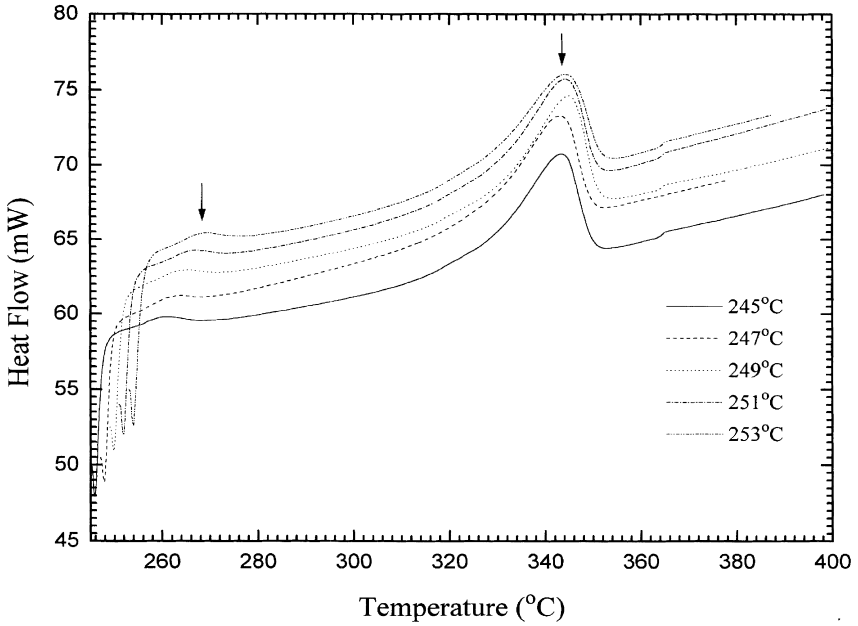

Fig. 1. D.s.c. diagrams for crystalline PEEK. The samples were kept at different temperatures for 30 min when heated from 100°C to 400°C, all portions of d.s.c. scans below the keeping temperatures are omitted.

unchanged as a result of the post-annealing treatment, while the lower peak appears as a movable feature. With an increase in annealing time as discussed below, the low endothermic peak shifts slightly to a higher peak temperature. It is likely that a melting of the low endothermic peak and subsequent recrystallization process to form the higher melting endothermic material has occurred in the post-annealing.

Fig. 2 shows the d.s.c. scans of semicrystalline PEEK subject to crystallization at 220° for 24 h. The record was interrupted at 245°C and kept at the same temperature for different periods of time. After 1 min, a third peak appeared in the intermediate of the d.s.c. diagrams. The position of the third peak (indicated by II in Table 1) shifts to a higher temperature and the heat of fusion of the third peak increases with time (see Table 1). Further experiments show that below 1 min, such as 30 s, no other melting peak emerges during the post-heating scan, in addition to the upper melting peak. Accordingly, during the d.s.c. continuous scans with slightly high scanning rate, such as 20 deg min^{-1}, only a melting process of the thinner crystal populations occurred, and the recrystallization process was not found.

Summarizing the results above, when the semi-crystalline

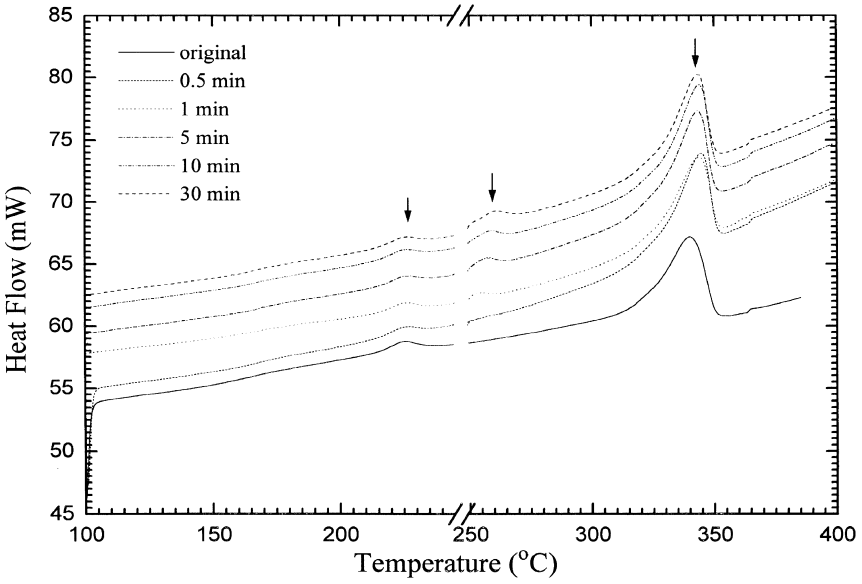

Fig. 2. D.s.c. diagrams of PEEK subjected to crystallization at 220°C for 24 h. The scans were interrupted and kept at 245°C for different times.

Table 1
Thermal properties of semi-crystalline PEEK samples. The d.s.c. heating scans were interrupted and kept at 245°C for different periods of time

Time (min)	T_m (deg.)			ΔH_f (J g^{-1})		
	I	II	III	I	II	III
0.5	224	—	344	3.1	—	43.0
1	224	253	343	3.1	1.2	41.8
5	224	256	343	3.1	2.3	42.3
10	224	257	343	3.1	2.3	43.8
30	224	260	343	3.1	2.7	43.4

samples are subjected to heating, a portion of crystallite was melted and transformed into metastable melt which is far from the equilibrium molten state and can recrystallize just above the lower melting temperature only if there is enough time to rearrange the molecular chains in such circumstances. The metastable melt may exist between the thicker lamellae, and the further recrystallization of these melts could occur among these main lamellae. Further TEM, WAXD observations in the following section may support the proposal that a metastable melt was obtained during the d.s.c. heating trace.

3.2. Morphological feature observed after isothermal crystallization

Thin films of PEEK crystallized at 220°C for 24 h from the glassy state show a typical spherulitic morphology consisting of narrow edge-on lamellae (see Fig. 3). A part of a spherulite with lamellar crystals is shown in Fig. 4. Two or more layers of lamellar crystals are frequently stacked together. It should be noted that this sample possesses two endothermic peaks in the initial d.s.c. heating scan as shown in Fig. 2. After being heated to 245°C and quenched into liquid nitrogen, the sample only shows the high endothermic peak in the d.s.c. heating scan. In TEM observations on PEEK samples with the same thermal history, individual lamellar crystals exhibiting a longer period are found, as shown in Fig. 5. This result seems to indicate that before the partial melting process, two kinds of lamellar crystals exist. When the temperature increases to 245°C, the thinner

Fig. 3. TEM micrograph of PEEK spherulite crystallized from the glassy state at 220°C for 24 h. Scale bar is 500 nm.

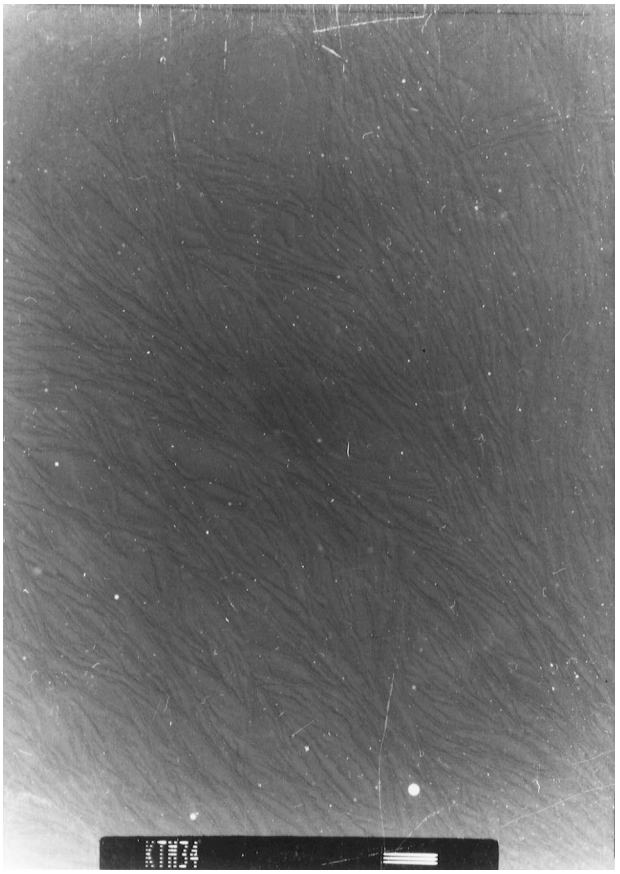

Fig. 4. TEM observations of PEEK edge-on lamellar morphology in spherulites crystallized from the glassy state at 220°C for 24 h. Scale bar is 200 nm.

Fig. 5. TEM observations of PEEK edge-on lamellar morphology in spherulites crystallized from the glassy state at 220°C for 24 h. After the melting of the thinner lamellae. Scale bar is 200 nm.

lamellae melts, due to its lower stability. The remaining lamellar crystals may thicken during the heating process. Therefore, a population of less stable lamellar crystals may be responsible for the low endothermic peak.

The structural evidence is provided by WAXD experiments. The crystallinity of all samples can be determined according to the usual method. Fig. 6 shows the WAXD patterns obtained before and after the partial melting process as described in the Experimental section. The PEEK sample after being heated to 245°C and then quenched into liquid nitrogen shows a slightly lower diffraction intensity than the original one. Table 2 lists the crystallinity of the PEEK samples before and after the partial melting process at 245°C. It should be noted that the crystallinity drops slightly after partial melting and then increases with the post-annealing time at 245°C. Combining the d.s.c. results as discussed in the foregoing section, we can draw the conclusion that a metastable melt can be obtained during the d.s.c. heating trace in-between the two endothermic peaks and that the metastable melt of PEEK can subsequently recrystallize to form the higher melting temperature materials.

Further evidence is given by SAXS experiments. Long periods can be determined after the Lorentz correction of the background-corrected scattering intensity. Table 2 lists the long periods of PEEK crystallized at different crystallization temperatures before and after the partial melting of the samples at 245°C also. It is found that after partial melting, the long period shows a clear increase as compared with the initial value. This result is consistent with the crystal morphological observation using TEM. One possible explanation is the melting of the thermodynamically less stable, thinner lamellae in-between the more stable, thicker lamellae. As a result, the residual thicker lamellae increases

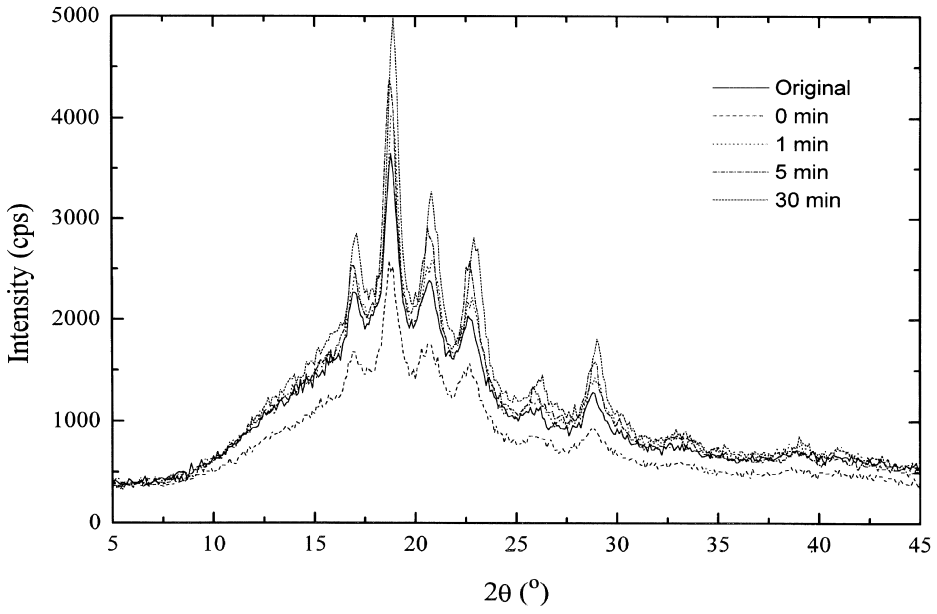

Fig. 6. WAXD patterns of PEEK samples before and after partial melting and post-annealing at 245°C process.

Table 2
Crystallinity of the PEEK samples determined from WAXD data and long period determined from the small angle X-ray scattering maximum in Lorentz-correction using Bragg's law before and after partial melting and post-annealing process

Sample	Original (220°C, 24 h)	After heating to and keeping at 245°C			
		0 min	1 min	5 min	30 min
X_t (%)	41.0	37.0	38.0	39.5	40.2
L (nm)	9.5	10.0	11.2	11.7	14

the long period. This seems to indicate that the long periods observed after partial melting are determined by the temperature at which the heating process for the partial melting stops. At 245°C, the more stable lamellae may thicken. Accordingly, the long periods determined by SAXS do increase after partial melting, but are not exactly double that of the original long periods. This demonstrates that the population of the thermodynamically less stable lamellae is relatively small compared with that of the thicker lamellae.

As discussed above, the metastable melt formed during d.s.c. heating scan to between the low and the high melting peaks can recrystallize to transform into the higher temperature materials. Thus, the crystallization kinetics of these metastable melt may be determined by general d.s.c. method, which will be discussed in the next section.

3.3. Crystallization kinetics of metastable PEEK melts

The well-known Avrami equation was used to describe the crystallization kinetics

$$X_t = 1 - \exp(-kt^n) \quad (2a)$$

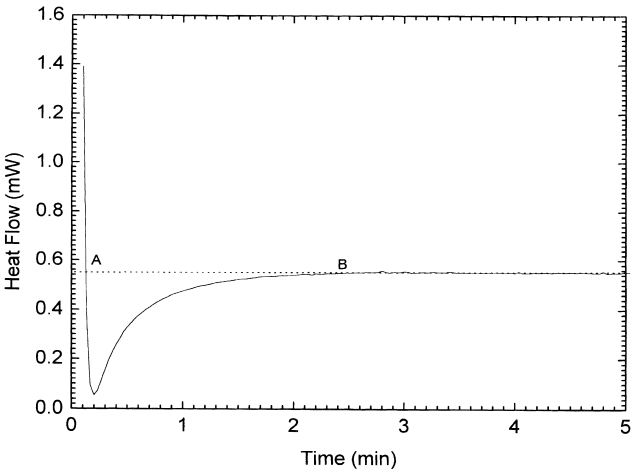

Fig. 7. Time dependence of the heat flow for the isothermal crystallization of PEEK from the metastable melt at 247°C. The crystallization curves at other temperatures are omitted here.

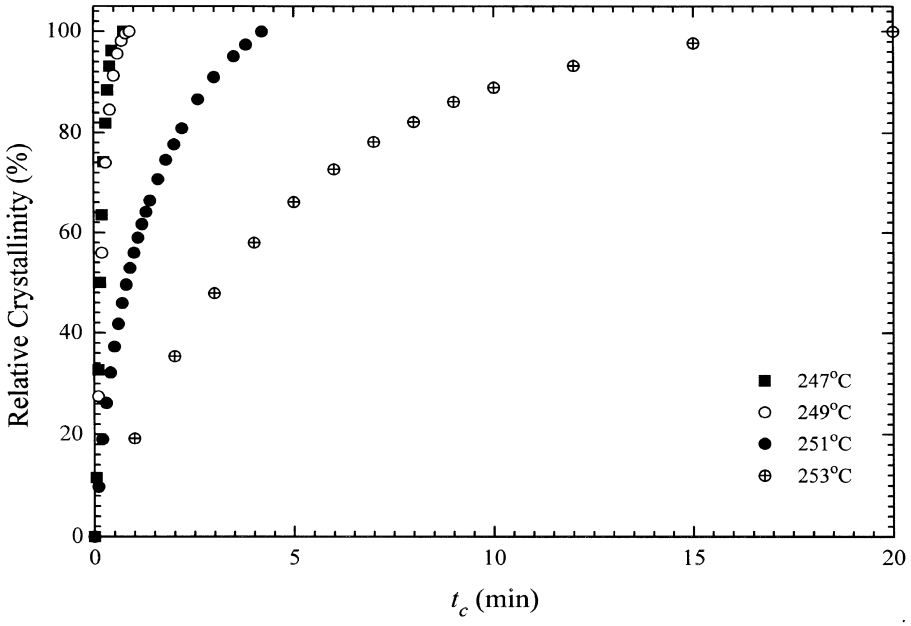

Fig. 8. The time dependence of the relative crystallinity index (X_t) for the crystallization of PEEK metastable melts after heating to a temperature in-between the two endothermic peaks.

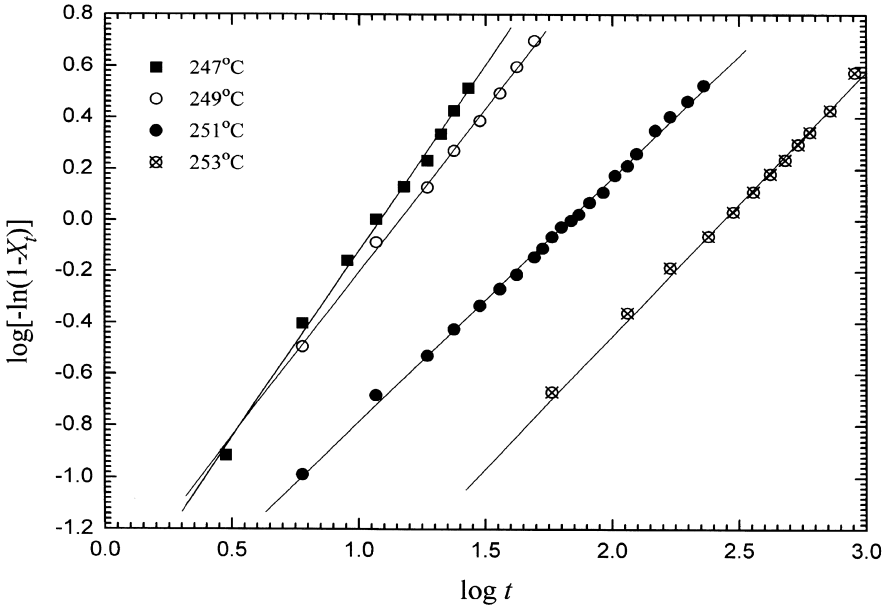

Fig. 9. Avrami plot for the crystallization of PEEK from its metastable melt.

or

$$\log[-\ln(1-X_t)] = \log k + n \log t \quad (2b)$$

where X_t is the relative crystallinity at time t as described in the Experimental section, k is the crystallization rate constant depending on nucleation and growth rates, and n is the Avrami crystallization exponent depending upon the nature of nucleation and growth geometry of the crystals. Fig. 7 presents the heat flow change for the isothermal crystallization from the metastable melt at 247°C. The starting point cannot be identified clearly, which may be indicated by point A in this case for the clarification of calculation of the relative crystallinity; the maximum is reached fast and the crystallization slows down beyond the point B. In our case, the measurement is terminated when no more heat flows from the sample. Thus, the total heat flow, $\int_0^\infty (dH_t/dt)dt$ as used in Eq. (1), is denoted as the total area under the crystallization endotherm from point A to point B in Fig. 7 at the crystallization temperature, 247°C. Of course, the whole procedure from the data acquisition to the partial and the total area integration is carried out in the microcomputer equipped with the d.s.c. system. The variations of the relative crystallinity index (X_t) as a function of time are shown in Fig. 8. All isotherms have a partial sigmoidal shape, not typical of the full sigmoidal shape of the polymer crystallization behaviour. Crystallization isotherms were generated from these isotherms by plotting $\log[-\ln(1-X_t)]$ against $\log t$.

The Avrami plots for the isothermal crystallization of the metastable melt from semicrystalline PEEK sample shown in Fig. 9 revealed a straight line for each temperature yielding a single value of slope. Crystallization kinetic parameters from the analysis are summarized in Table 3. From the slopes of the Avrami plots, the exponents were easily obtained as 1.0–1.4, which were found to vary only slightly with the isothermal crystallization temperatures used. These values of n for isothermal crystallization of metastable melts are different from the exponent for isothermal crystallization of regular melt of PEEK, which are generally between 2.5 and 3.0. The n values of approximately 3.0 for regularly melt crystallization of PEEK suggests that the initiation process is simultaneous and the growth of crystals is most likely spherulitic. On the other hand, the exponent of approximately 1.0 for the crystallization of metastable melt suggests that the mechanism of this crystallization is completely altered. The exponent of around 1.0 suggests an initiation process of heterogeneous nucleation and probably linear crystal growth. This phenomenon is in good agreement with our previous works on PET [23].

The Avrami parameter k is assumed to be thermally activated and can be used to determine an activation energy for crystallization [7,24,25]. Thus, it can be approximately described by [7]

$$k^{1/n} = k_0 \exp(-\Delta E/RT) \quad (3)$$

where k_0 is a temperature-independent pre-exponential factor, ΔE is activation energy, and T is the absolute temperature. The linear regression of the experimental data of

Table 3
Crystallization kinetic parameters for PEEK metastable melt. T_c: temperature of isothermal crystallization; ΔE: activation energy of crystallization.

T_c (deg.)	n	k (s^{-n})	ΔE (kJ mol^{-1})
247	1.4	2.69×10^{-2}	
249	1.3	3.39×10^{-2}	1196
251	0.95	1.82×10^{-2}	
253	1.03	3.09×10^{-3}	

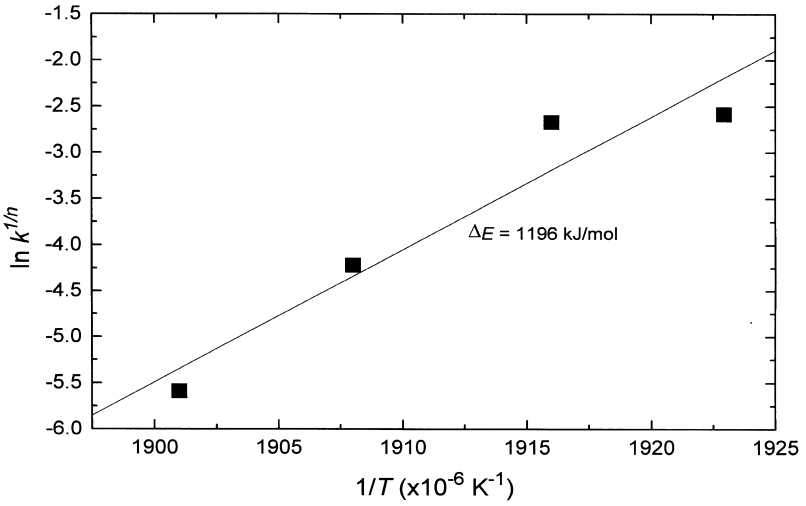

Fig. 10. Plot of ln k as a function of 1/T for the isothermal crystallization of PEEK from the metastable melt, from which the crystallization activation energy can be estimated.

ln k against l/T determines $\Delta E/R$ (see Fig. 10). The magnitude of the activation energy was found to be 1196 kJ mol^{-1} for isothermal crystallization from the metastable melt. This activation energy is comparable to the value of 1400 kJ mol^{-1} reported by Kemmish and Hay [24] for isothermally cold crystallization and lower than the value of 2500 kJ mol^{-1} calculated by Bas et al. [25] for the crystallization from the regular melt. It is clear that the activation energy is strongly dependent upon the nucleation type. The activation energy for cold crystallization from the glassy state is lower than that for isothermal melt crystallization. The nuclei existing in the PEEK glassy samples play an important role in the isothermal crystallization of PEEK. Our activation energy of crystallization for PEEK metastable melt is comparable to that for isothermally cold crystallization, which shows the important role of the existing main lamellae in the isothermal crystallization of PEEK metastable melt.

4. Conclusion

Double melting behaviour is a common phenomenon during the heating scans of d.s.c. for semicrystalline polymers, i.e. PEEK etc. containing rigid segmental links. Stacked edge-on orientational lamellae crystal morphology after isothermal crystallization of thin amorphous PEEK films have been observed. Some minor stacked lamellae disappear after partial melting occurs by heating the sample to a temperature above the low melting peak. This has been associated with the double endothermic behaviour seen in d.s.c. heating scans and supported by WAXD and SAXS measurements. The minor low temperature peak is attributed to the melting of thinner lamellae formed through secondary crystallization among the first formed thicker lamellae. The thinner crystallites can be transformed into metastable melt through the heating of the semicrystalline samples. This metastable melt may recrystallize immediately and formed new thicker lamellae among the existing main lamellae only if there is enough time for the chains in the melt to reorganize. The crystallization of these melts abides by the classic theory of phase transformation proposed by Avrami, and a value of $n \approx 1.0 \sim 1.4$ is obtained. An Arrhenius plot can be applied to determine activation energy of the isothermal crystallization for PEEK metastable melt. The activation energy thus obtained, 1196 kJ mol^{-1}, is comparable to that for isothermally cold crystallization of PEEK in the literature and implies the important role of nuclei, the existing main lamellae.

Acknowledgements

This research was supported, in part, by the National Natural Science Foundation of China and the National Key Projects for Fundamental Research ‘Macromolecular Condensed State’, The State Science and Technology Commission of China. The authors thank Professor Stephen Z.D. Cheng of the University of Akron for his critical and helpful comments. S.S. Tan also express his warm thanks to Mrs. Xiaoguang Zhao for her kind help in the manuscript preparation. The d.s.c. measurements were taken by Professor Y.C. Qi and Mrs. L.X. Li.

References

[1] Hsiao BS, Gardner KH, Cheng SZD. J Polym Sci: Part B: Polym Phys 1994;32:2585.
[2] Gardner KH, Hsiao BS, Matheson RR Jr, Wood BA. Polymer 1992;33:2483.
[3] Wang J, Cao J, Chen Y, Ke Y, Wu Z, Mo Z. J Appl Polym Sci 1996;1999:61.
[4] Blundell DJ. Polymer 1987;28:2248.
[5] Verma RK, Hsiao BS. Trends Polym Sci 1996;4:312.

[6] Cheng SZD, Cao MY, Wunderlich B. Macromolecules 1986;19:1868.
[7] Cebe P, Hong SD. Polymer 1986;27:1183.
[8] Bassett DC, Olley RH, Raheil IAM. Polymer 1988;29:1745.
[9] Lee Y, Poter RS, Lin JS. Macromolecules 1989;22:1756.
[10] Jonas AM, Russell TP, Yoon DY. Macromolecules 1995;28:8491.
[11] Ko TY, Woo EM. Polymer 1996;37:1167.
[12] Medellin-Rodriguez FJ, Phillips PJ. Polym Eng Sci 1996;36:703.
[13] Zhang Z, Zeng H. Polymer 1993;34:3648.
[14] Blundell DJ, Osborn BN. Polymer 1983;24:953.
[15] Hsiao BS, Sauer BB, Verma RK, Zachmann HG, Seifert S, Chu B, Harney P. Macromolecules 1995;28:6931.
[16] Jonas AM, Russel TP, Yoon DY. Macromolecules 1995;28:8491.
[17] Hsiao BS, Gardner KH, Wu DQ, Chu B. Polymer 1993;34:3986.
[18] Hsiao BS, Gardner KH, Wu DQ, Chu B. Polymer 1993;34:3996.
[19] Fougnies C, Damman P, Villers D, Dosiere M, Koch MHJ. Macromolecules 1997;30:1385.
[20] Fougnies C, Damman P, Dosiere M, Koch MHJ. Macromolecules 1997;30:1392.
[21] Lattimer MP, Hobbs JK, Hill MJ, Barham PJ. Polymer 1992;33:3971.
[22] Strobl GR. Acta Crystallogr A 1970;26:367.
[23] Tan S, Su A, Li W, Zhou E. Macromol Rapid Commun 1998;19:11.
[24] Kemmish DJ, Hay JN. Polymer 1985;26:905.
[25] Bas C, Grillet AC, Thimon F, Alberola ND. Eur Polym J 1995;31:911.